X-~~612-69~~-374
PREPRINT

NASA TM X-63657

VARIATIONS IN ELECTRIC FIELDS FROM POLAR ORBITING SATELLITES

N. C. MAYNARD
J. P. HEPPNER

AUGUST 1969

GSFC

GODDARD SPACE FLIGHT CENTER
GREENBELT, MARYLAND

VARIATIONS IN ELECTRIC FIELDS FROM
POLAR ORBITING SATELLITES

N. C. Maynard
J. P. Heppner

August 1969

Presented at the Summer Advanced Study Institute, "Earth's Particles and Fields, 1969", Santa Barbara, California, August 4-15, 1969.

INTRODUCTION

The advent of techniques to measure electric fields in the ionosphere and above has put new emphasis on the questions of what electric fields exist in the ionosphere and magnetosphere and how they vary. The probe technique using long antennas on rockets and satellites (AGGSON, 1969) is useful in studying the spatial variations of electric fields, complimenting the study of temporal variations using the motions of barium ion clouds (FOPPL, et al, 1967; LUST and HAERENDEL, 1970; WESCOTT, 1970, and WESCOTT, et al. 1969).

Electric fields in the magnetosphere have been theoretically postulated as convection patterns derived from the distributions of ionospheric currents (AXFORD and HINES, 1961; for a review see AXFORD, 1969). These assume that the electric field is related to the convective velocity by:

$$\underline{E} = -\underline{v} \times \underline{B}$$

and that the conductivity along magnetic field lines is infinite allowing them to be equipotentials. While these patterns are useful in estimating gross behavior, it has been noted (HEPPNER, 1969), that the smaller scale irregularity structure must be understood to explain many questions regarding auroral forms and morphology, and it was suggested that this structure is related to the presence of larger scale d.c. electric fields. It is the purpose here to further define the characteristics of the electric fields inferred from OVI-10 measurements using preliminary data from OGO-6 (launched in June 1969) which substantiates the OVI-10 data on spatial irregularities and waves in the ELF - VLF regime.

OGO-6 is also providing highly accurate measurement of large scale d.c. electric fields, but presentation of these results (other than figures regarding typical magnitudes) will have to await the merging of measurements with orbit and vehicle orientation data.

THE EXPERIMENTS

The probe technique (AGGSON, 1969) using long cylindrical antennas has been used to measure electric fields from d.c. to low VLF frequencies on both OVI-10 and OGO-6. Briefly, the experiment monitors the potential difference between two axial antennas using a high input impedance voltmeter. This potential difference, Ø, is related to the electric field by

$$\emptyset = (\underline{E} + \underline{v} \times \underline{B}) \cdot \underline{d}$$

where $\underline{v}$ is the velocity of the vehicle and $\underline{d}$ is the vector distance between the antenna midpoints.

Since the $\underline{v} \times \underline{B}$ field tends to mask the desired ambient fields, it has to be subtracted to observe the ambient field. As $\underline{v}$ and $\underline{B}$ are well known, and/or measured, the accuracy of the subtraction is primarily dependent on knowing the vehicle orientation. The principal effect of the $\underline{v} \times \underline{B}$ term is the limitation it places on the sensitivity of the d.c. measurement in that the telemetry scale must accomodate a $\underline{v} \times \underline{B}$ range of plus and minus several hundred millivolts per meter in addition to the ambient field strength. This becomes a severe handicap in looking for variations of less than several millivolt per meter. Thus, for observing small scale irregularities a capacitor coupled logarithmic amplifier (log channel) with a 60 second time constant is used. For even greater sensitivity at higher frequencies, the RMS level of signals in the region between 3 Hz and 4 kHz was measured by separating the range into three bands in the case of OVI-10 (3 - 30 Hz, 30 - 300 Hz and 300 - 3000 Hz) and five bands in OGO-6 (4 - 16 Hz, 16 - 64 Hz, 64 - 256 Hz, 256 - 1024 Hz and 1 - 4 kHz).

OVI-10, launched in December, 1966, (648 by 776 km orbit with a 93.4° inclination), had 51-foot antennas aligned along the local vertical for use in the gravity gradient stabilization of the satellite. Each antenna was insulated over the inner 19-feet to move the active element away from spacecraft interference fields. Unfortunately, a short on one antenna prevented d.c. measurements from being made; however, the a.c. measurements have proved very useful. Since the configuration of the booms was not normal due to the short, and the gravity gradient stabilization was weak, the direction of the component measured is ambiguous.

OGO-6 was launched in June, 1969, into a more eliptical polar orbit (400 to 1600 km with an inclination of 82°). The 30-foot antennas extended from each solar array and were insulated on the inner 15 feet (to move the active element away from spacecraft fields such that the baseline d was 20 meters). Stabilization is such that the antennas are always perpendicular to the normal to the earth and vary in orientation from north-south in the dawn-dusk plane to east-west in the noon-midnight plane. Results presented here are all from the dawn-dusk plane, hence the component of field being measured is essentially north-south.

OBSERVATIONS

1. Low Frequency Irregularities. The data from OVI-10 indicated a usually distinct boundary as one passed from the equator toward the pole where the 3 - 30 Hz channel rose sharply above the noise (HEPPNER, 1969; HEPPNER, et al., 1968). It was also noted that the activity in the log channel increased in this region, usually between 60 and 75° INL,

indicating the possible presence of strong spatially varying d.c. electric fields. The 3 - 30 Hz signal, in the majority of cases, reached peak intensity at slightly higher latitudes than the region of maximum auroral occurrence and decreased in the central region of the polar cap.

Since the satellite is moving in the vicinity of 8 km/sec. the most probable conclusion as to the source of the signal were that the satellite was moving through magnetic field aligned irregularity structures typically 0.2 to 2 Km in width. In interpreting the OVI-10 data there was the possibility that the detected signal could have resulted from electron density irregularities as a consequence of the probe asymmetry caused by the short circuit to one of the axial probes. Thus, the measurements might not have truly represented electric field irregularities. It was assumed, however, that such an irregularity structure in the electron density would have to be accompanied by a nearly identical electric field structure to maintain current continuity in the E-region -- subject, of course, to the assumption that the irregularity structure extended downward to the E-region. Additional confidence in the assumption that the irregularities did extend to the E-region was later gained from the observation of highly similar and simultaneous striation structure in Ba^{+} clouds above 200 Km and aurora near 100 Km (WESCOTT, et al., 1969 AGU). Another factor which indicated that OVI-10 was measuring electric field irregularities was the observation of conjugate agreement in the minimum latitude of occurrence, noted later in this paper. The OGO-6 results provide strong evidence that the OVI-10 assumptions were correct.

The same characteristics response is seen in preliminary data from OGO-6. Figure 1 depicts data from two spectrum channels (4 - 16 Hz and 256 - 1024 Hz) and from the log and d.c. channels in the northern hemisphere from near the equator to the auroral regions. The onset of activity in the 4 - 16 Hz channel occurs near and slightly before the obvious activity in the log and d.c. channels. The level quickly rises from the background to 10 to 30μvolts/meter RMS with spikes up to several hundred μvolts/meter. The log channel recorded variations of the order of 15 mvolt/meter. Of particular interest is the essentially complete absence of the irregularity signal at low latitudes. The signal level is below 0.4 μv/meters. Figure 2 shows a more active pass across the southern auroral regions from dawn to dusk. In the vicinity of 65° INL, the 4 - 16 Hz channel increased from around 10 μv/meter to several hundred μv/meter near the onset of activity in the d.c. channel. The activity is depressed over the polar cap and returns again on the high latitude side of the evening auroral region. The peaks of the 4 - 16 Hz signal typically are several hundred μv/meter and occasionally go as high as several mv/meter.

The overall distribution of this irregularity signal can be seen from the OVI-10 data. Figure 3 shows the locations in latitude and magnetic time of the peak intensities encountered on each polar pass. Kp values at these times are noted for three levels of activity by the symbols used. Although a shift to lower latitudes with increasing Kp is apparent in peak intensities, it appears most clearly in plots of the average minimum latitude of occurrence(See HEPPNER, 1969).

As a consequence of the nearly infinite conductivity along magnetic field lines above 600 Km, electric field irregularities should appear magnetically conjugate in both hemispheres. Figure 4 represents an attempt to look at the conjugacy of the lowest latitude of occurrence. Obviously, as sampling of opposite hemispheres involves time separations of 25-40 or 55-70 minutes and the orbit is tilted relative to the earth's magnetic axis, good comparison cannot be made for most of the orbits. However, by restricting comparisons to those cases where the magnetic local times in opposite hemispheres are within one hour, it becomes quite clear that conjugacy exists. Figure 4 shows all the OVI-10 cases fulfilling the one hour criteria where good data was available from both hemispheres on the same orbit.

The electric field picture presented here is one of a small scale irregularity structure superimposed on the irregular d.c. field seen at auroral latitudes. While this structure is only a few percent or less in magnitude of the larger variations, its importance can be inferred by it being characteristic of the high latitude ionosphere, always being present with d.c. fields. Interpreting this low frequency signal as a spatial variation, one notes that the length scale is similar to that of auroral rays and the striations observed in Barium clouds (WESCOTT, et al., 1969). It has been suggested by them that an $\underline{E} \times \underline{B}$ plasma instability (e.g. SIMON, 1963) could be the cause of the observed irregularities.

2. D.C. and Slow Variations. As final orbit and vehicle attitude information was not available the $\underline{v} \times \underline{B}$ variations could not be removed from the d.c. channel of Figures 1 and 2. However, this variation is a slowly varying smooth curve; hence, rapid variations seen in the 60 to 80^{o} INL regions can be interpreted as varying d.c. fields. The magnitude of these north-south directed fields is in the 10 to 100 mv/meter range and is in good agreement with the rocket results from both barium clouds (WESCOTT et al., 1969) and probes (AGGSON, 1969). One notes that the largest d.c. fields occur at the time of maximum activity in the 4 - 16 Hz channel, with the start of small variations commencing near the onset of the 4 - 16 Hz irregularity signal. D.C. fields have not been seen without

the presence of the 4 - 16 Hz signal.

3. ELF Electric Fields. The two higher spectrometer channels on OGO-6 tend to follow each other relatively closely. The 256 - 1024 Hz variations plotted in Figures 1 and 2 exemplify the general behavior in that they usually peak before the main onset of the 4 - 16 Hz signal. The poleward decrease in signal occurs before the decrease in the 4 - 16 Hz signal, usually in the regions of strong d.c. fields. Typically, field strengths vary between 50 and 100 μv/meter, occasionally reaching several hundred μv/meter.

This is in good agreement with signal levels observed by OVI-10. Figure 5 shows the distribution of orbital segments where the signal intensity in the 300 - 3000 Hz band exceeded 1.0 or 2.8 millivolts. Taking 15 meters as the effective antenna length, this corresponds to rms values of 66 and 180 μvolts/meter, respectively. Although the data gaps between 2^h to 4^h and 14^h - 16^h limit complete comparison with TAYLOR and GURNETT'S (1968) plots of the diurnal distribution of these signals observed by means of the magnetic component it is clear from both the spatial-diurnal distribution and the magnitudes that these signals are propagating in the whistler mode. Thus, there is not any reason to view them as electrostatic waves.

REFERENCES

AGGSON, T. L.: 1969, Atmospheric Emissions, (Ed. by B. M. McCormac), Reinhold Publishing Corporations, N. Y., 305.

AXFORD, W. I.: 1969, Magnetospheric Physics, (Ed. by D. J. Williams and G. D. Mead) American Geophysical Union, Washington, D. C. 421.

AXFORD, W. I. and HINES, C. O.: 1961, Can. J. Phys. 39, 1433.

FÖPPL, H., HAERENDEL, G., HASER, L., LOIDL, J., LÜTJENS, P., LÜST, R., NIELZNER, F., MEYER, B., NEUSS, H. and RIEGER, E.: 1967, Plan. Space Sci. 15, 357-372.

HEPPNER, J. P.: 1969, Atmospheric Emissions,(Ed. by B. M. McCormac) Reinhold Publishing Corporations, N. Y., 251.

HEPPNER, J. P., AGGSON, T. L. and MAYNARD, N. C.: 1968, (Abstract) Symposium on the Physics of the Magnetosphere, Washington, D. C., Sept. 1968.

LÜST, R. and HAERENDEL, G.: 1970, this volume.

SIMON, A.: 1963, Phys. Fluids, 6, 382.

TAYLOR, W. L. and GURNETT, D. A.: 1968, J. Geophys, Res. 73, 5615.

WESCOTT, E. M.: 1970, this volume.

WESCOTT, E. M., STOLARIK, J. D. and HEPPNER, J. P.: 1969, J. Geophys. Res, 74, 3469.

WESCOTT, E.M., HEPPNER, J. P., STOLARIK, J. D., HALLIMAN, T., DAVIS, T. N. and ROMICK, G. J.: 1969, Rapid Ray Motions Through Barium Ion Clouds and Associated Auroras (Abstract) AGU Annual Meeting Washington, D. C., April.

Figure Captions

Figure 1: OGO-6 electric field data (June 12, 1969) depicting the latitude variation from near the equator to the auroral region at dusk in the northern hemisphere.

Figure 2: OGO-6 electric field data (June 13, 1969) showing the latitude variation in a dawn to dusk pass across the southern auroral and polar cap regions.

Figure 3: The location of the maxima in the 3-30 Hz irregularity signal from OV1-10 data as a function of invariant latitude and magnetic local time. Variation with Kp is denoted by the different symbols.

Figure 4: The degree of conjugacy of the minimum latitude of occurrence of the 3-30 Hz irregularity signal from OV1-10 data in invariant latitude-magnetic local time coordinates.

Figure 5: The distribution of regions where the RMS input to the 300-3000 Hz channel on OV1-10 exceeded 10^{-3}v. (approximately 66μv./m) and 2.8 x 10^{-3}v. (approximately 180μv./m) in the northern and southern hemispheres.

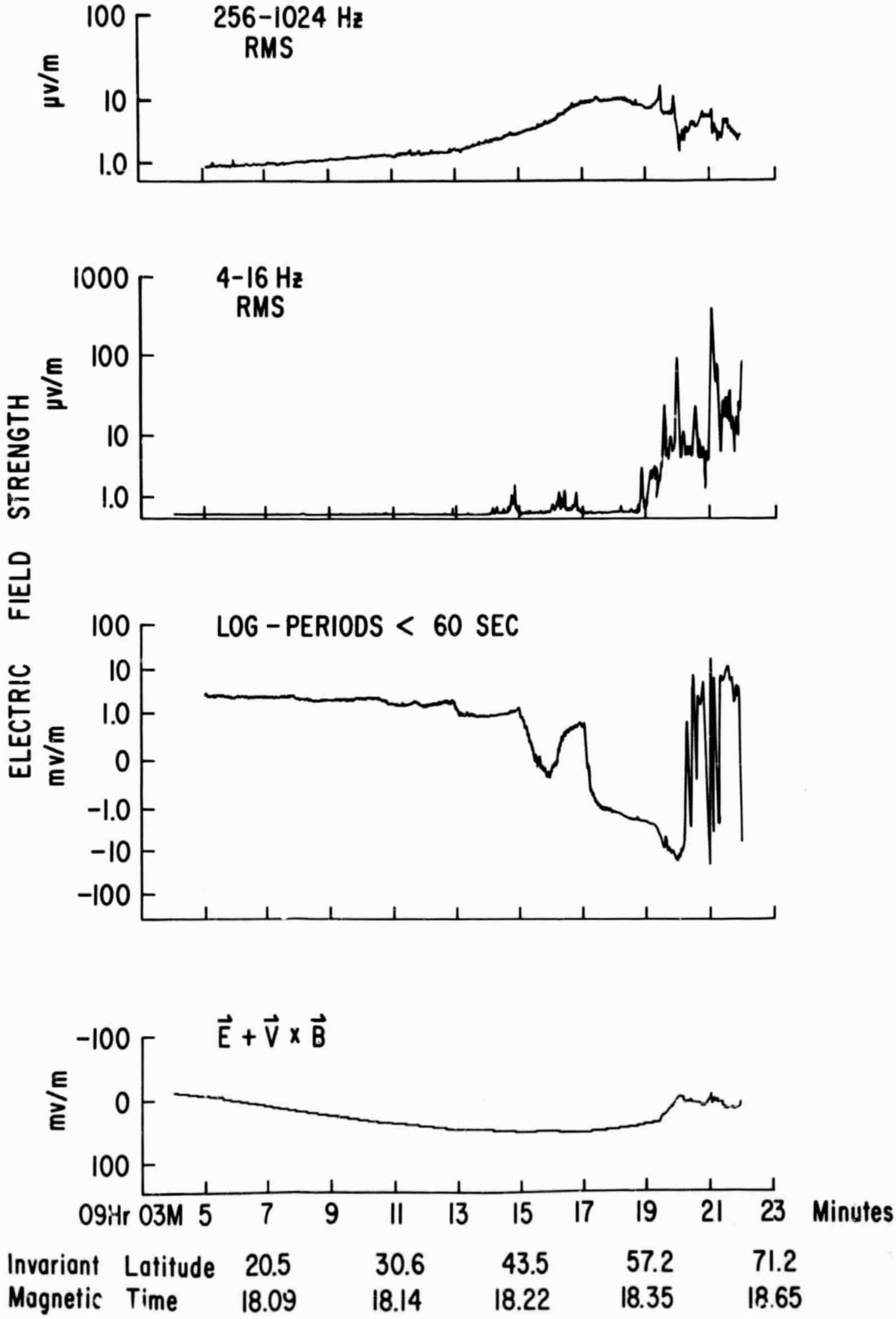
256-1024 Hz
RMS
μv/m
100
10
1.0
4-16 Hz
RMS
1000
100
10
1.0
ELECTRIC FIELD STRENGTH
μv/m
LOG - PERIODS < 60 SEC
mv/m
100
10
1.0
0
-1.0
-10
-100
$\vec{E} + \vec{V} \times \vec{B}$
mv/m
-100
0
100
09Hr 03M 5 7 9 11 13 15 17 19 21 23 Minutes
Invariant Latitude 20.5 30.6 43.5 57.2 71.2
Magnetic Time 18.09 18.14 18.22 18.35 18.65

FIGURE 1

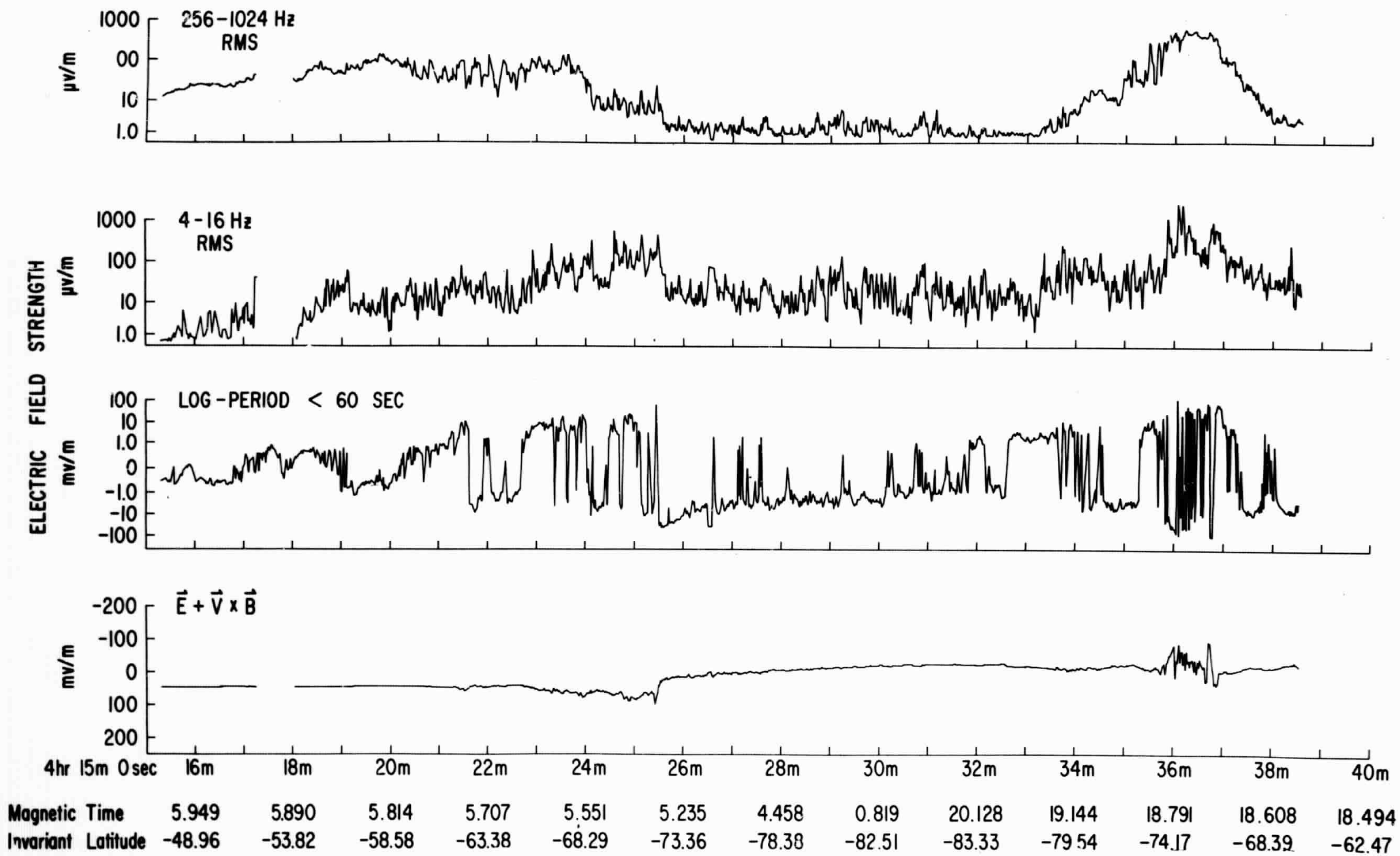

ELECTRIC FIELD STRENGTH
μv/m
1000
00
10
1.0
256-1024 Hz
RMS
μv/m
1000
100
10
1.0
4-16 Hz
RMS
mv/m
100
10
1.0
0
-1.0
-10
-100
LOG-PERIOD < 60 SEC
mv/m
-200
-100
0
100
200
E + V x B
4hr 15m 0sec
16m
18m
20m
22m
24m
26m
28m
30m
32m
34m
36m
38m
40m
Magnetic Time 5.949 5.890 5.814 5.707 5.551 5.235 4.458 0.819 20.128 19.144 18.791 18.608 18.494
Invariant Latitude -48.96 -53.82 -58.58 -63.38 -68.29 -73.36 -78.38 -82.51 -83.33 -79.54 -74.17 -68.39 -62.47

FIGURE 2

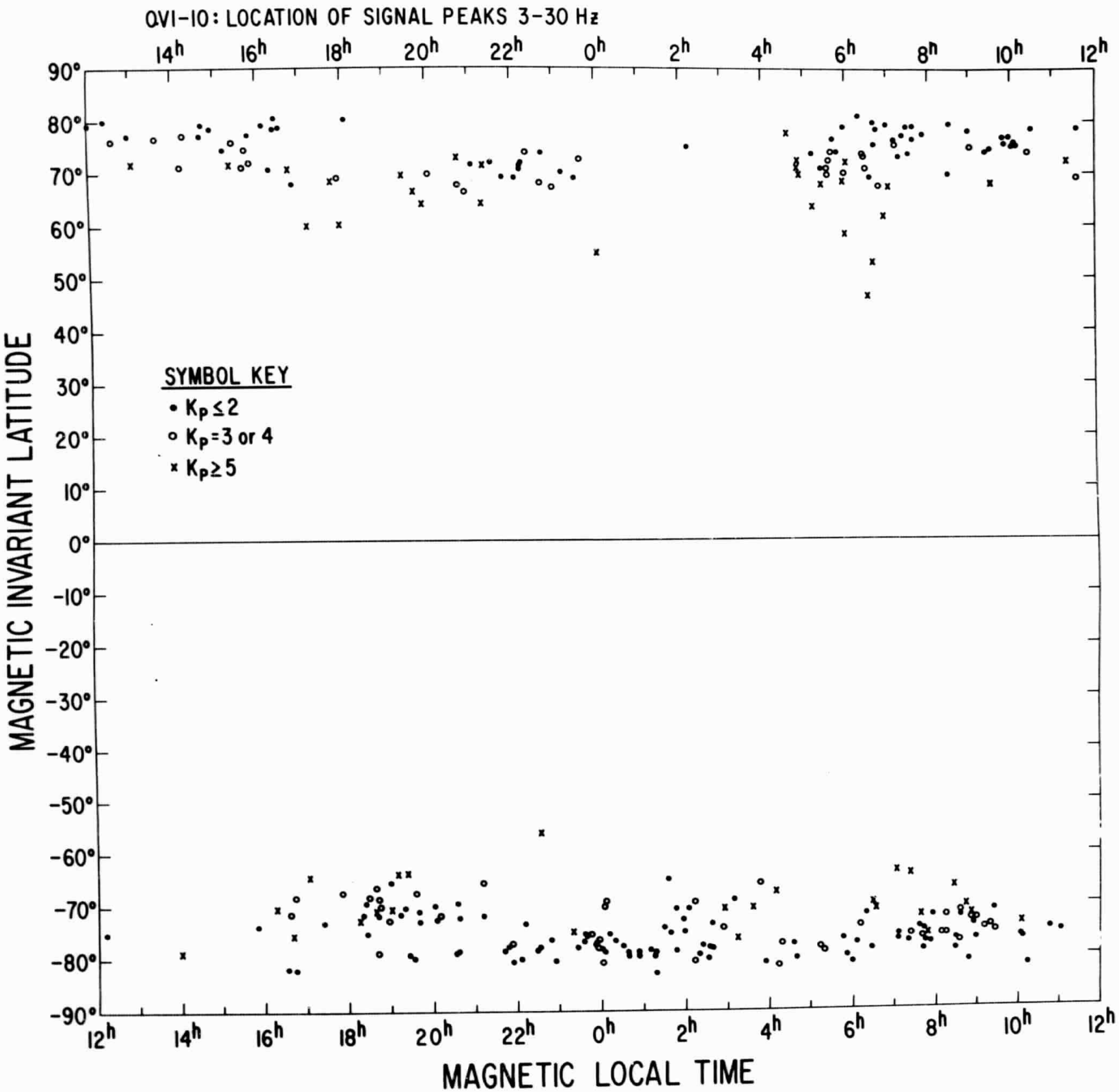

OVI-10: LOCATION OF SIGNAL PEAKS 3-30 Hz
MAGNETIC INVARIANT LATITUDE
MAGNETIC LOCAL TIME
90° 80° 70° 60° 50° 40° 30° 20° 10° 0° -10° -20° -30° -40° -50° -60° -70° -80° -90°
12h 14h 16h 18h 20h 22h 0h 2h 4h 6h 8h 10h 12h
SYMBOL KEY
• Kp ≤ 2
o Kp = 3 or 4
x Kp ≥ 5

FIGURE 3

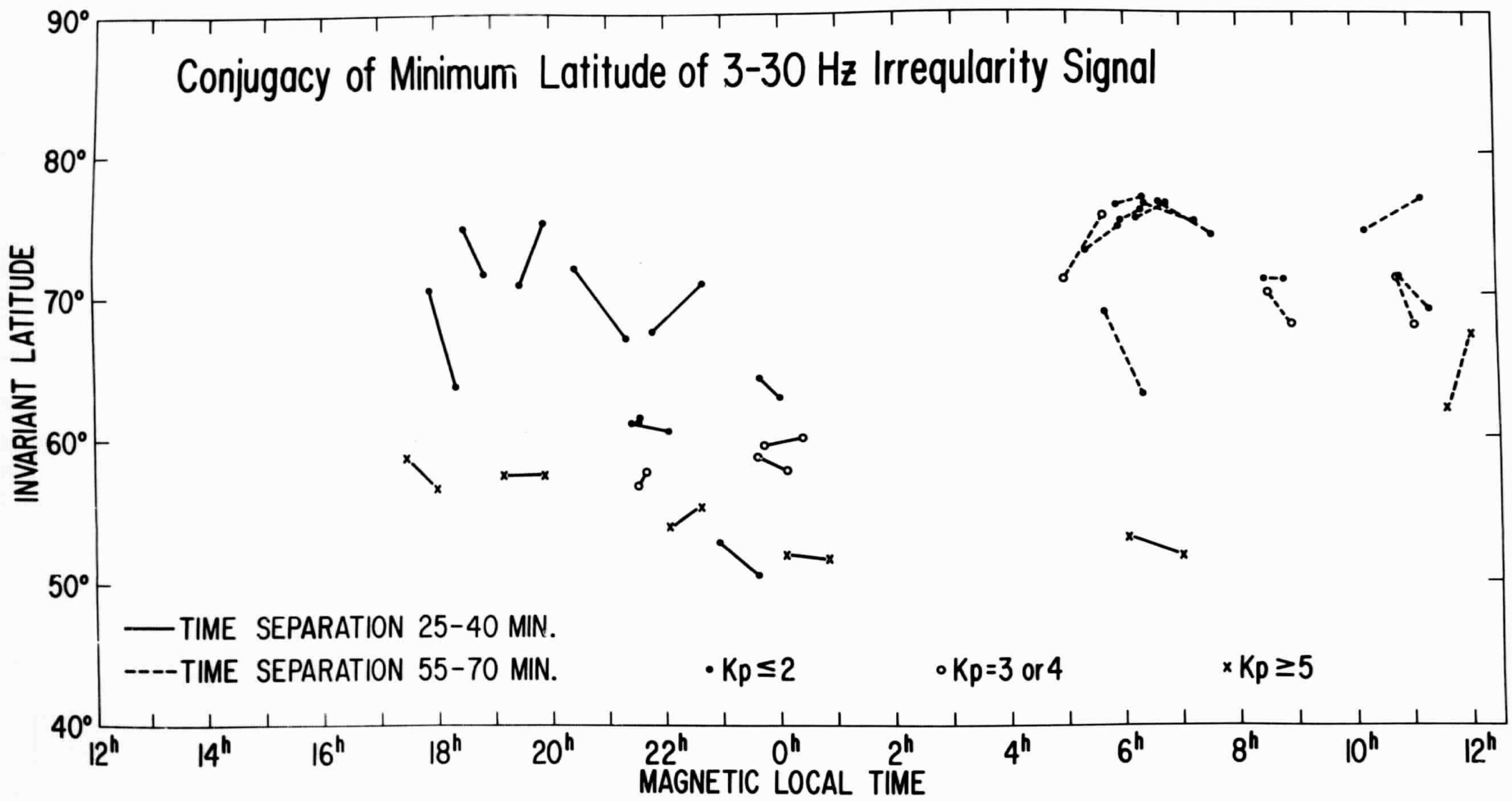
Conjugacy of Minimum Latitude of 3-30 Hz Irregularity Signal
90°
80°
70°
60°
50°
40°
INVARIANT LATITUDE
12h
14h
16h
18h
20h
22h
0h
2h
4h
6h
8h
10h
12h
MAGNETIC LOCAL TIME
—— TIME SEPARATION 25-40 MIN.
---- TIME SEPARATION 55-70 MIN.
• Kp≤2
∘ Kp=3 or 4
× Kp≥5

FIGURE 4

NORTH HEMISPHERE

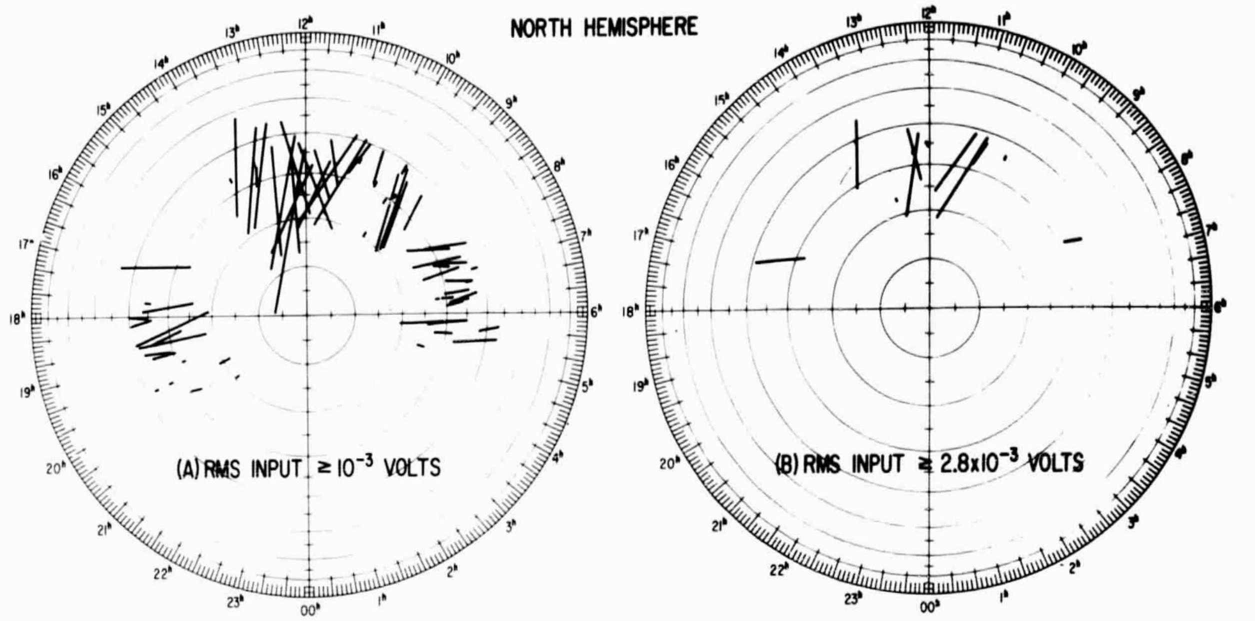

SOUTH HEMISPHERE

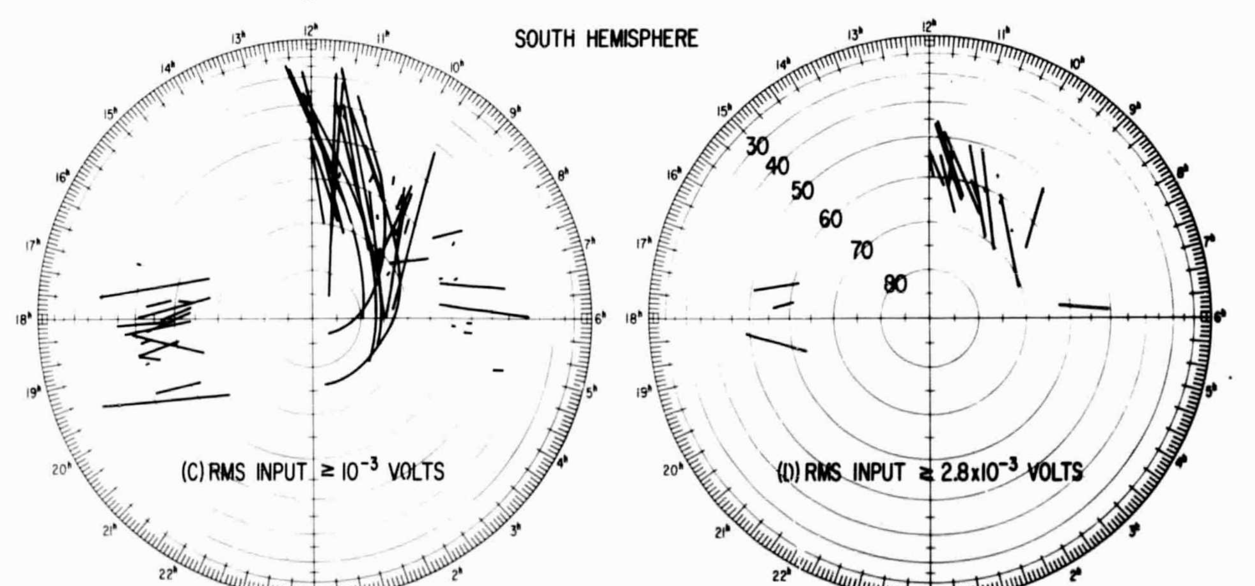

300-3000 Hz

FIGURE 5